Supporting Information

Rapid preparation of self-adhesive PAA ionic hydrogel using lignin sulfonate-Al^{3+} composite systems for flexible moisture-electric generators

Jinchao Zhang [a, 1], Jingshun Zhuang [a, 1], Lirong Lei [a], Yi Hou [a, *]

[a] State Key Laboratory of Pulp and Paper Engineering, South China University of Technology, Guangzhou, 510641, P.R. China

[*] Corresponding authors: Email address: ceyhou@scut.edu.cn (Yi Hou)

[1] Jinchao Zhang and Jingshun Zhuang contributed equally to this work.

Supplementary Figures

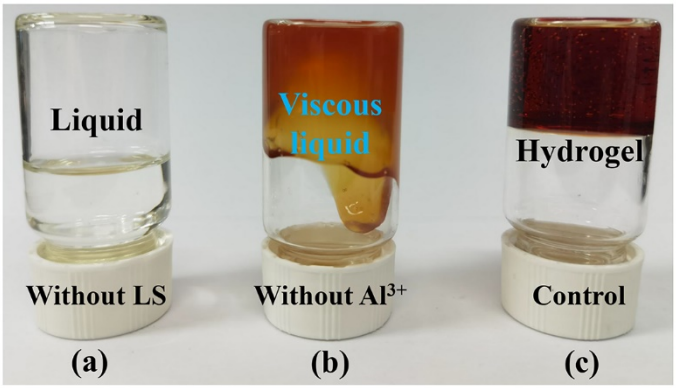

Fig. S1. Gelation of the various hydrogels triggered by different systems (room temperature). a) AA/APS/Al^{3+}. b) AA/APS/LS. c) AA/APS/Al^{3+}/LS.

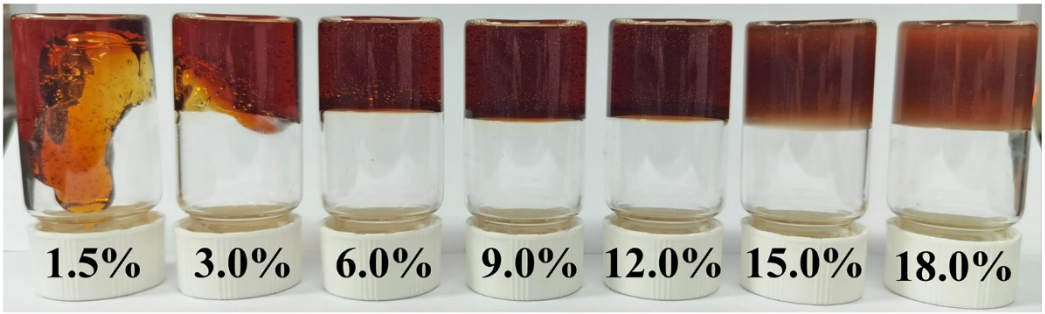

Fig. S2. Various hydrogels from different Al^{3+} contents (1.2 wt.% LS, 28.0 wt.% AA, and 0.25 wt.% APS).

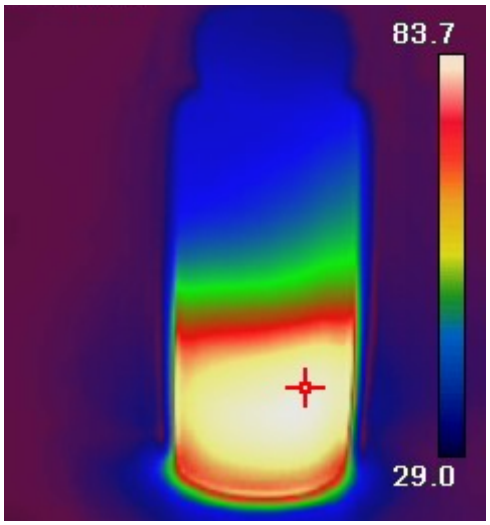

Fig. S3. Infrared thermal imaging photo of the reaction during the hydrogel preparation.

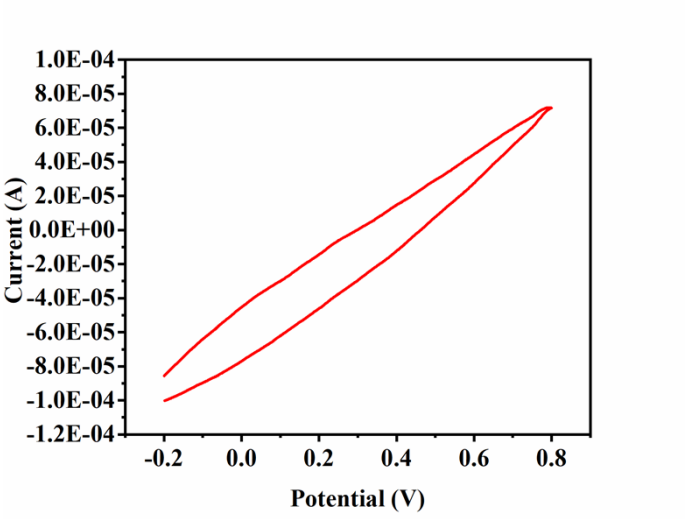

Fig. S4. CV curves of the LS working electrode in pure deionized water.

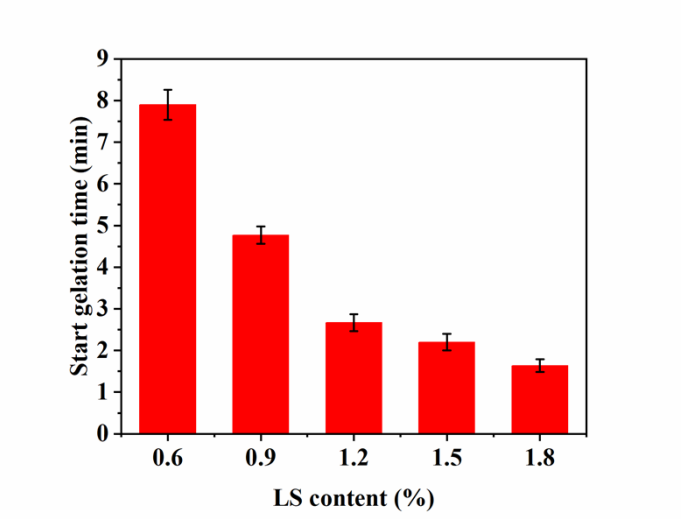

Fig. S5. Start gelation (exothermic) time of hydrogels with different LS contents (12.0 wt.% Al^{3+}, 28.0% AA, and 0.25% APS).

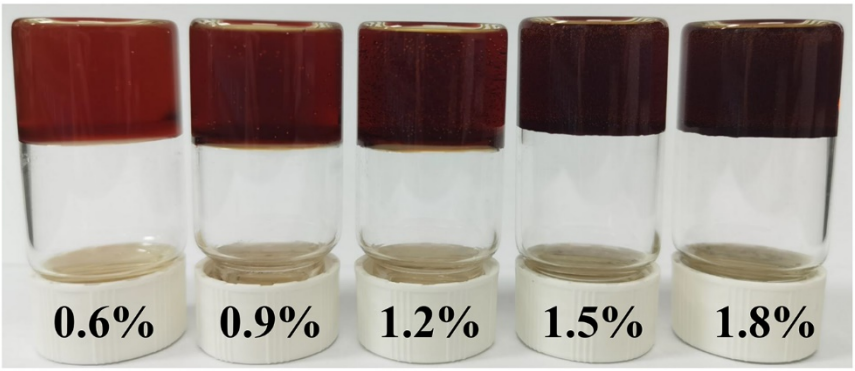

Fig. S6. Various hydrogels from different LS contents (12.0 wt.% Al^{3+}, 28.0 wt.% AA, and 0.25 wt.% APS).

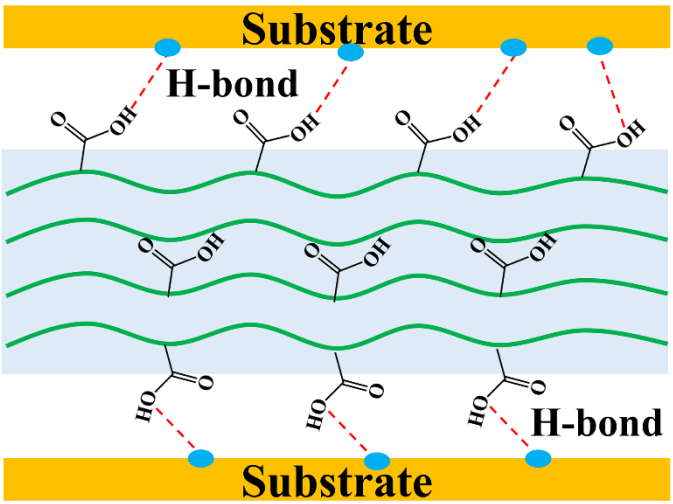

Fig. S7. The adhesion mechanism of the LS-Al^{3+}-PAA hydrogel.

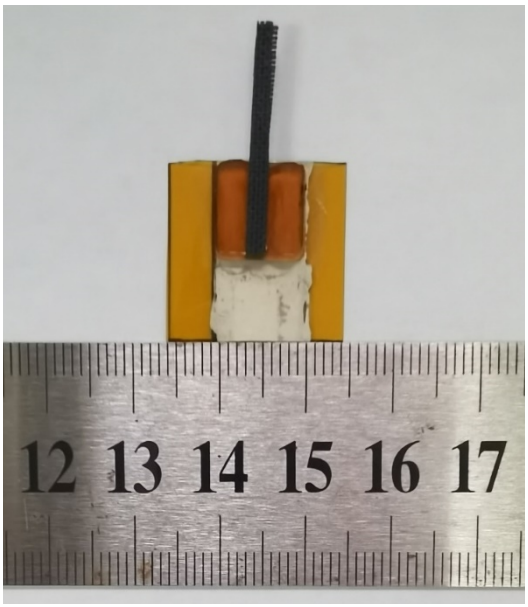

Fig. S8. The actual photograph of the HMEG device against a centimeter ruler.

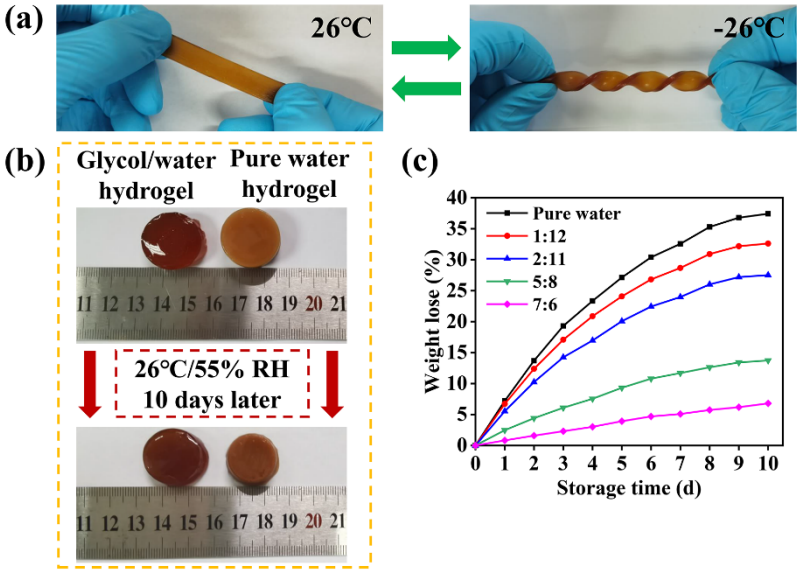

Fig. S9. a) Anti-freezing properties of the LS-Al^{3+}-PAA hydrogel. b) Comparison of moisture retention capacities of glycol/water and pure water hydrogels. c) Weight losses of the LS-Al^{3+}-PAA hydrogels with different ratios of glycol to water measured at predetermined intervals (temperature of about 26 ℃ and relative humidity of about 55%).

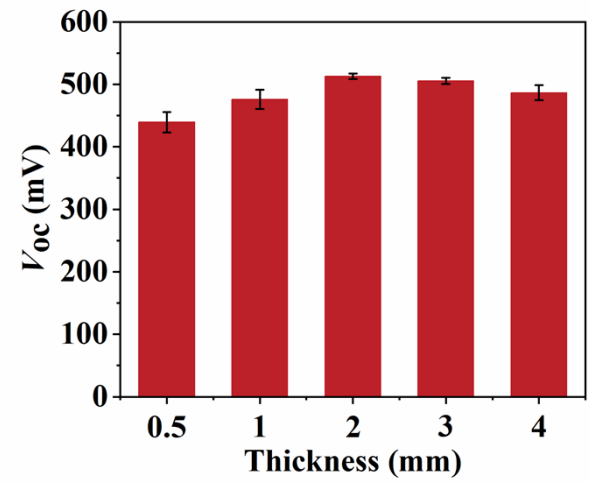

Fig. S10. Effect of hydrogel thickness on *V*oc (12.0 wt.% Al^{3+}, 0.9 wt.% LS).

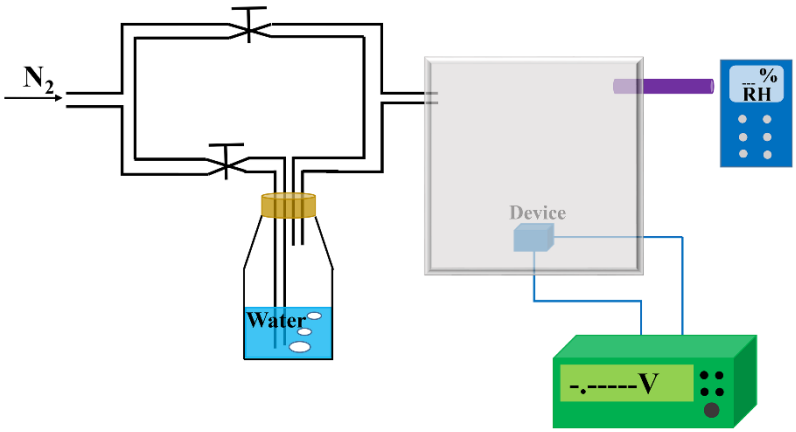

Fig. S11. Schematic diagram of the lab-made moisture circulating system.

The humidity was controlled by adjusting the ratio of wet nitrogen (moisture) flow and dry nitrogen flow. When the bottom valve was turned up and the upper valve was turned down, the nitrogen passed through water and carried moisture towards the CMEG to achieve high humidity that could be monitored with a hygrometer beside the CMEG. On the contrary, when the upper valve was turned up and the bottom valve was turned down, pure dry N_2 brought a low humidity environment.

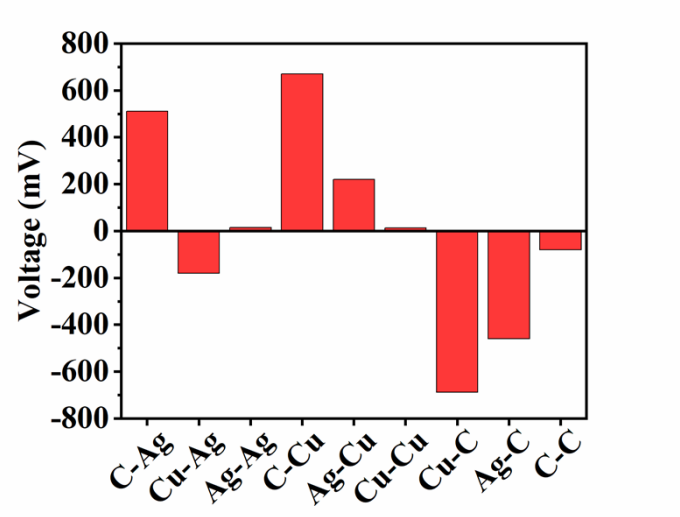

Fig. S12. The voltage output of the HMEG with different electrode materials, from left to right: carbon cloth-silver paste, copper foil-silver paste, silver mesh-silver paste, carbon cloth-copper foil, silver mesh-copper foil, copper foil-copper foil, copper foil-carbon cloth, silver mesh-carbon cloth and carbon cloth-carbon cloth. The left side of the combination was the upper electrode, and the right side was the lower electrode. For example, C-Ag, where C was the upper electrode and Ag was the lower electrode. The positive terminal of the test circuit was connected to the upper electrode and the negative terminal was connected to the lower electrode.

The electrodes have a significant effect on the output performance of the HMEG device. In the asymmetrical electrode material system containing carbon, the output voltage of the device with Cu electrodes was higher than that of the device with Ag electrodes. When the two electrodes of the device were exchanged up and down, the polarity of the potentials were also exchanged accordingly, while the absolute value of the output voltage remained basically unchanged. The potential generation of the device was affected by the activity of the electrode material. The side of the metal electrode with higher activity exhibited a lower potential, which may be due to the interaction between the water molecules and the metal electrodes. In addition, the lower voltage output of the devices with symmetrical electrode system may be attributed to the supercapacitance of these two symmetrical electrodes.

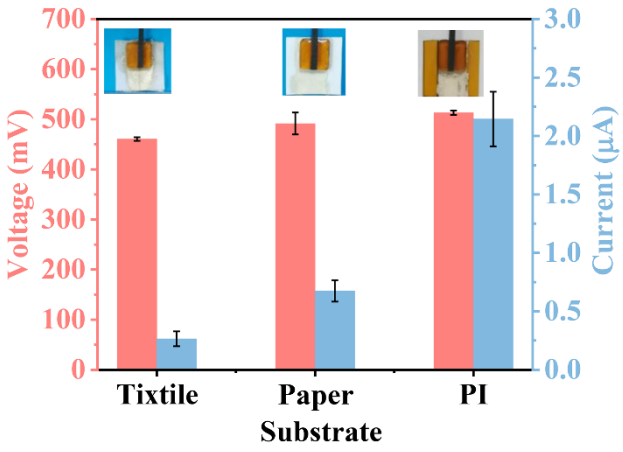

Fig. S13. The V_{oc} and I_{sc} generated by hydrogels on different flexible substrates.

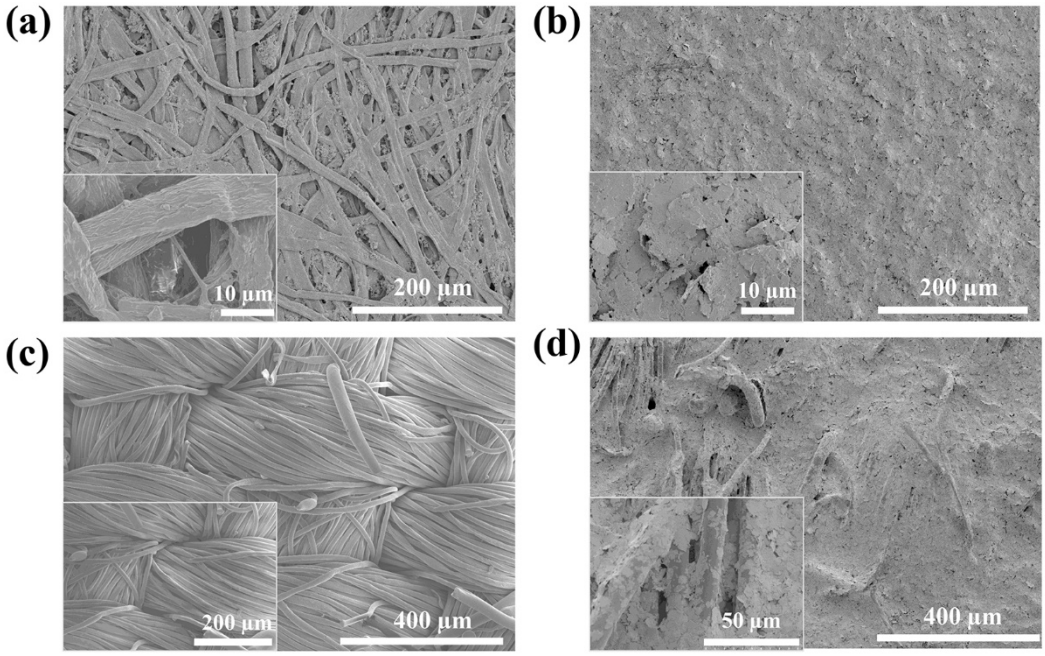

Fig. S14. SEM images of different flexible substrates. (a) Paper, (b) Paper coated with conductive silver paste, (c) Fabric, (d) Fabric coated with conductive silver paste.

Supplementary Tables

Table S1. The content of Al^{3+} of Al^{3+}-LS-g-PAA hydrogels

Samples	$AlCl_3 \cdot 6H_2O$ (g)	AA (g)	APS (mg)	LS (g)	Glycol/water ratio
3.0 wt.% Al^{3+}	0.3	2.8	25	0.12	5:8
6.0 wt.% Al^{3+}	0.6	2.8	25	0.12	5:8
9.0 wt.% Al^{3+}	0.9	2.8	25	0.12	5:8
12.0 wt.% Al^{3+}	1.2	2.8	25	0.12	5:8
15.0 wt.% Al^{3+}	1.5	2.8	25	0.12	5:8

Table S2. The content of LS of Al^{3+}-LS-g-PAA hydrogels

Samples	$AlCl_3 \cdot 6H_2O$ (g)	AA (g)	APS (mg)	LS (g)	Glycol/water ratio
0.6 wt.% LS	1.2	2.8	25	0.06	5:8
0.9 wt.% LS	1.2	2.8	25	0.09	5:8
1.2 wt.% LS	1.2	2.8	25	0.12	5:8
1.5 wt.% LS	1.2	2.8	25	0.15	5:8
1.8 wt.% LS	1.2	2.8	25	0.18	5:8

Table S3. The ratio of glycol to water of Al^{3+}-LS-g-PAA hydrogels

Samples (Glycol to water ratio)	$AlCl_3 \cdot 6H_2O$ (g)	AA (g)	APS (mg)	LS (g)	Deionized water (g)	Glycol (g)
0	1.2	2.8	25	0.09	6.5	0
1:12	1.2	2.8	25	0.09	6	0.5
2:11	1.2	2.8	25	0.09	5.5	1
5:8	1.2	2.8	25	0.09	4	2.5
7:6	1.2	2.8	25	0.09	3	3.5

Table S4. Peak species, binding energies, and peak area ratios (%) of the high-resolution C1s spectra of LS and APS-oxidized LS.

Peak species	C-C(H)	C-O(C-OH)	C=O	C=O / C-O(C-OH) ratio
Binding energy (eV)	281.7	283.0	285.8	-
LS	63.85%	34.39%	1.76%	0.05
APS-oxidized LS	42.44%	43.02%	14.54%	0.34

Table S5. Comparison reported hydrogels and hydrogel-based moist-electric generators with our work.

Components of hydrogel	Open-circuit Voltage (V_{oc})	Short-circuit Current (I_{sc})	Preparation time	Stretchability (Max)	Adhesive	Green cross-linker	Heat input	Reference
MXene-PAM	13 mV	-	>12 h	-	-	No	No	1
PVA/CNTs/ Tannic acid	80 mV	-	~30 h	350 %	-	-	Yes	2
MXene-CNCs-tamarind gum-PAM	164 mV	-	>5.5 h	2000 %	-	No	Yes	3
PVA/CNFs	170 mV	-	> 18 h	450%	-	Yes	Yes	4
PVA/Lignin	226 mV	-	> 50 h	250%	-	No	Yes	5
Sodium alginate/ lignosulfonate/PAA	306 mV	-	> 15 h	436%	Yes	No	Yes	6
PAA/Lignin/ Al^{3+}	**550 mV**	**3.28 µA**	**<1 h**	**500%**	**Yes**	**Yes**	**No**	**This work**

"-": Not available or not mentioned in references, "PAM": Polyacrylamide, "PVA": Polyvinyl alcohol, "CNCs": Cellulose nanocrystals, "CNFs": Cellulose nanofibrils, "PAA": Polyacrylic acid.

Supplementary Video S1. A voltage of about 2.5 V generated by connecting five devices in series under a normal ambient laboratory environment.

References

[1] Q.H. Wang, X.F. Pan, X.P. Wang, H.L. Gao, Y.B. Chen, L. Chen, Y.H. Ni, S.L. Cao, X.J. Ma, Spider web-inspired ultra-stable 3D Ti3C2TX (MXene) hydrogels constructed by temporary ultrasonic alignment and permanent in-situ self-assembly fixation, Compos. Pt. B-Eng. 197 (2020) 8.

[2] P. He, J.Y. Wu, X.F. Pan, L.H. Chen, K. Liu, H.L. Gao, H. Wu, S.L. Cao, L.L. Huang, Y.H. Ni, Anti-freezing and moisturizing conductive hydrogels for strain sensing and moist-electric generation applications, J. Mater. Chem. A 8(6) (2020) 3109-3118.

[3] P. He, R.S. Guo, K. Hu, K. Liu, S. Lin, H. Wu, L.L. Huang, L.H. Chen, Y.H. Ni, Tough and super-stretchable conductive double network hydrogels with multiple sensations and moisture-electric generation, Chem. Eng. J. 414 (2021) 9.

[4] X.F. Pan, Q.H. Wang, R.S. Guo, S.L. Cao, H. Wu, X.H. Ouyang, F. Huang, H.L. Gao, L.L. Huang, F. Zhang, L.H. Chen, Y.H. Ni, K. Liu, An adaptive ionic skin with multiple stimulus responses and moist-electric generation ability, J. Mater. Chem. A 8(34) (2020) 17498-17506.

[5] Y. Zhang, A. MohebbiPour, J.C. Mao, J.H. Mao, Y.H. Ni, Lignin reinforced hydrogels with multi-functional sensing and moist-electric generating applications, Int. J. Biol. Macromol. 193 (2021) 941-947.

[6] C.L. Fu, J.K. Lin, Z.W. Tang, L.H. Chen, F. Huang, F.G. Kong, Y.H. Ni, L.L.

Huang, Design of asymmetric-adhesion lignin reinforced hydrogels with anti-interference for strain sensing and moist air induced electricity generator, Int. J. Biol. Macromol. 201 (2022) 104-110.